CHEMISTRY OF MATERIALS

pubs.acs.org/cm

Article

Transformation of One-Dimensional Linear Polymers into Two-Dimensional Covalent Organic Frameworks Through Sequential Reversible and Irreversible Chemistries

Dongyang Zhu, Xiaoyi Li, Yilin Li, Morgan Barnes, Chia-Ping Tseng, Safiya Khalil, Muhammad M. Rahman, Pulickel M. Ajayan, and Rafael Verduzco*

Cite This: *Chem. Mater.* 2021, 33, 413–419

Read Online

ACCESS | Metrics & More | Article Recommendations | Supporting Information

ABSTRACT: Covalent organic frameworks (COFs) are crystalline porous materials linked by dynamic covalent bonds. Dynamic chemistries enable the transformation of an initially amorphous network into a porous and crystalline COF. While dynamic chemistries have been leveraged to realize transformations between different types of COFs, including transformations from two-dimensional (2D) to three-dimensional (3D) COFs and insertion of different linking groups, the transformation of linear polymers into COFs has not yet been reported. Herein, we demonstrate an approach to transform linear imine-linked polymers into ketone-linked COFs through a linker replacement strategy with triformylphloroglucinol (TPG). TPG first reacts through dynamic chemistry to replace linkers in the linear polymers and then undergoes irreversible tautomerism to produce ketone linkages. We have analyzed the time-dependent transformation from the linear polymer into COF through powder X-ray diffraction, Fourier-transform infrared spectroscopy (FT-IR), and scanning electron microscopy (SEM) to understand the transition and substitution mechanisms. This work demonstrates another route to produce COFs through sequential reversible and irreversible chemistries and provides a potential approach to synthesizing COFs through the solution processing of linear polymers followed by transformation into the desired COF structure.

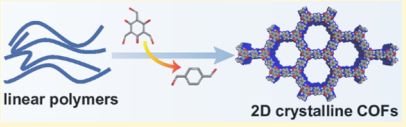

INTRODUCTION

Covalent organic frameworks (COFs) are emerging crystalline and porous materials linked by dynamic covalent bonds.[1−4] Their structure, porosity, and topology can be precisely controlled through the selection of the precursor monomers, enabling molecular-level control over pore size, pore chemistry, and pore functionality.[4] COFs are therefore highly promising for applications including gas storage and separation, water treatment, photocatalysis, electrochemical sensors, and energy storage.[1,2,4]

Most COFs are synthesized using dynamic, reversible chemistries, which enable network restructuring and crystallization.[5,6] For example, the dynamic Schiff-base reaction has been widely employed to construct imine COFs[2] and mechanistic studies demonstrated that these COFs are formed through an error-correcting process where the initially formed amorphous polymer networks form crystalline and porous materials through the re-organization of the dynamic imine bonds.[7] The dynamic nature of imine linkages also enables the postsynthetic linker substitution of covalent organic polymers (COPs) or COFs to yield novel crystalline COFs. For example, Zhao and co-workers developed a linker-replacement approach to produce COFs bearing three different kinds of pores.[8] Yaghi and co-workers constructed oxazole- and thiazole-linked frameworks through the addition of appropriately substituted linkers into the imine-COFs after synthesis.[9] In 2018, Zhao and co-workers synthesized crystalline imine-COFs starting from amorphous imine-linked COPs by the addition of different aldehyde monomers.[5] They subsequently reported a linker-substitution strategy to achieve the transformation of imine-COPs to imide-COFs as well as the conversion of imide-COPs to imine-COFs.[6] Linker replacement has also proven to be a powerful strategy to produce COFs with improved crystallinity and hierarchical architecture. Dichtel and co-workers significantly improved the crystallinity of β-ketoen-amine-linked COFs via the monomer exchange of imine-linked COFs.[10] Horike and co-workers produced COFs with core−shell architectures by partial linker substitution of the starting COFs.[11] Very recently, Han and co-workers realized the structural transformation between large-pore 3D COF (COF-320) and small-pore 3D COF (COF-300) and dimensional conversion of 3D COFs to 2D COFs through postsynthetic linker exchange.[12] Yan and co-workers also used a linker exchange strategy to synthesize two amino-functionalized imine COFs that were inaccessible through alternative synthetic pathways.[13] These studies demonstrate the value of linker exchange strategies in the synthesis of new COFs and in providing alternative synthetic routes to produce target COFs.

Received: November 1, 2020
Revised: December 15, 2020
Published: December 31, 2020

https://dx.doi.org/10.1021/acs.chemmater.0c04237
Chem. Mater. 2021, 33, 413−419

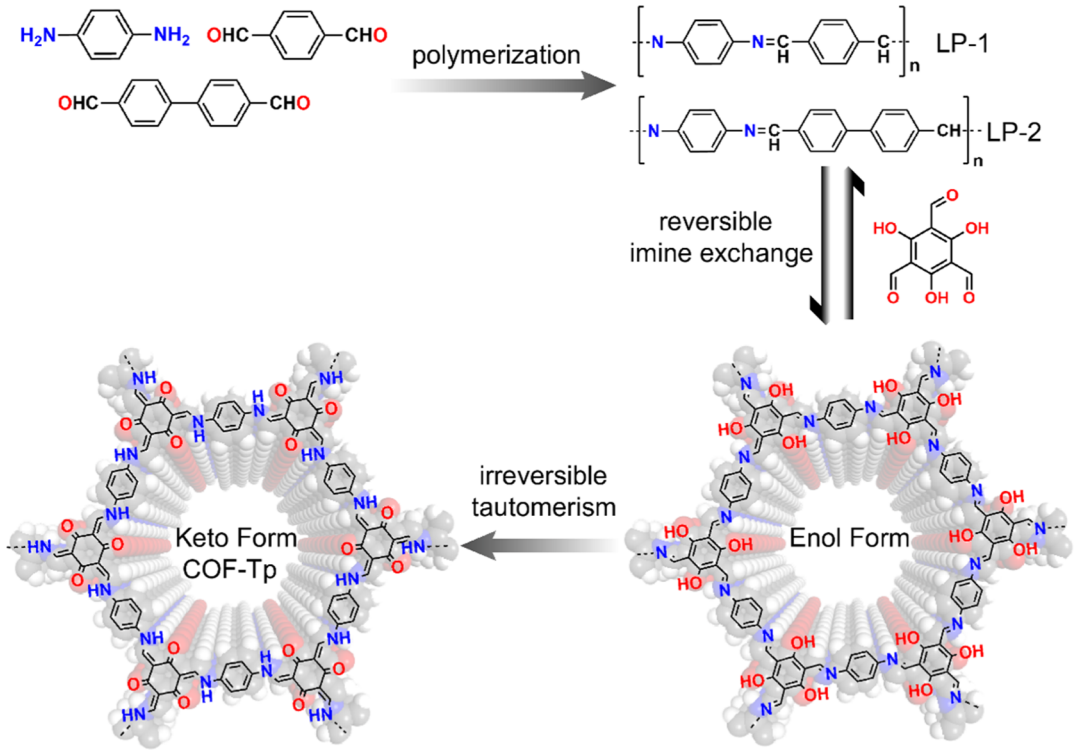

Figure 1. Synthetic scheme for the synthesis of COF-Tp through a linker replacement strategy.

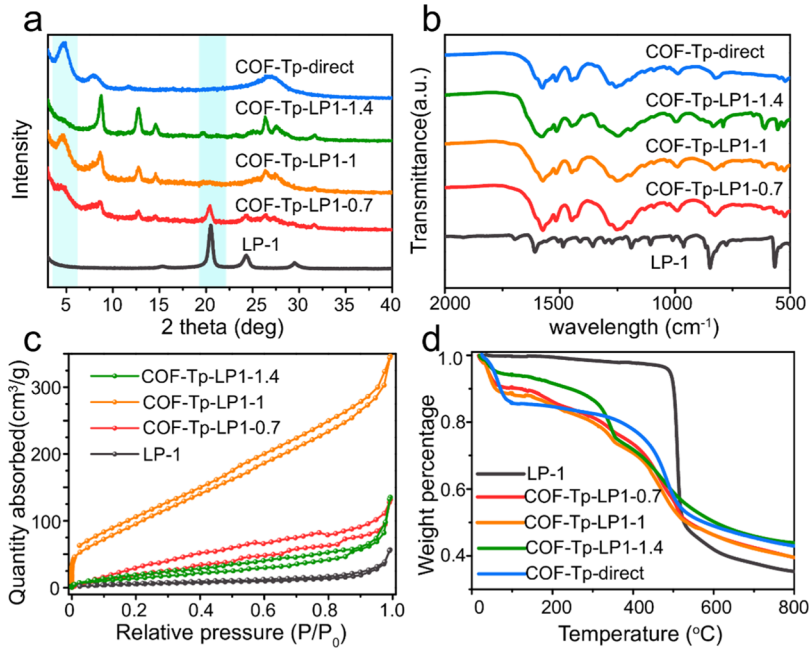

Figure 2. Characteristics of LP-1 and COF-Tp synthesized directly (blue trace) or through transformation of LP-1 samples (red, yellow, and green traces). (a) PXRD, (b) FT-IR, (c) nitrogen sorption isotherms, and (d) TGA analysis of samples.

The combination of reversible and irreversible chemistries has also been recently employed to construct ultra-stable and functional COFs. Banerjee and co-workers reported a series of ultra-stable COFs by first producing imine COFs with enol functional groups that subsequently tautomerized to form ketones, resulting in a COF with excellent stability toward both acids and bases.[14] The first reversible reaction step enabled error correction and crystallization, and the irreversible tautomerism transformed the enol form into the more stable keto form of the COF. Banerjee and co-workers further produced a series of β-ketoenamine COFs using an organic terracotta process in seconds[15] and synthesized porous thin films of this type of COFs through the self-assembly of COF nanospheres.[16] Furthermore, Han et al.,[17] Sun et al.,[18] and Yang et al.[19] also used a combination of reversible and irreversible chemistries to produce chiral COFs, bifunctional COFs, and carbonyl acid-decorated COFs, respectively.

https://dx.doi.org/10.1021/acs.chemmater.0c04237
Chem. Mater. 2021, 33, 413−419

Herein, we report a novel strategy to convert linear imine polymers into 2D COFs through sequential reversible and irreversible chemistries (Figure 1). We first synthesized linear imine-linked polymers (LP-1 & LP-2, Figure 1). Next, we performed a linker replacement reaction using 2,4,6-triformylphloroglucinol (TPG), which we hypothesized would replace the linking groups in the linear polymers and produce a 2D COF with more stable β-ketone linkages as a result of tautomerization of the enol functional groups to the more thermodynamically stable ketone groups (Figure 1).[3,14,20] We studied the effect of stoichiometry on the conversion from the linear polymer to COF and found successful transformation and excellent yields for an equimolar ratio of TPG to the starting aldehyde linker present. We also found higher crystallinities and surface areas for the transformed COF produced compared to the same COF synthesized directly from small molecular reagents. This work demonstrates the successful transformation of linear polymers into COFs and can potentially lead to new solution processing approaches for COF precursors that can be subsequently transformed into crystalline COFs.

RESULTS AND DISCUSSION

The linear polymer LP-1 was synthesized by the polycondensation of *p*-phenylenediamine (PDA) and terephthaladehyde (TPA) under solvothermal reaction conditions[21] (see details in the Materials and Methods section). The isolated product was an orange powder insoluble in many common solvents, including dimethyl sulfoxide (DMSO), N N-dimethylformamide (DMF), 1,4-dioxane, tetrahydrofuran (THF), acetone, acetonitrile, chloroform, and methanol. LP-1 was a semicrystalline linear polymer with diffraction peaks under powder X-ray diffraction (PXRD) analysis at 15.31, 20.51, 24.28, and 29.54° (Figure 2a), consistent with a previous study.[21] FT-IR analysis (Figure 2b) revealed an absorption peak at 1619 cm^{-1}, characteristic of an imine bond formed from the condensation of amine and aldehyde monomers.[21,22] LP-1 exhibited a nitrogen sorption isotherm characteristic of nonporous materials with a very low surface area (Figure 2c), and a slight increase of nitrogen uptake was observed at $P/P_0 < 0.01$, indicating LP-1 did not possess any micropores. We also synthesized COF-Tp using a direct synthesis route by the reaction between PDA and TPG, following methods previously reported.[14] Briefly, PDA and TPG were dissolved in a mixture of dioxane and mesitylene (v/v, 1/1) and reacted at 120 °C for 3 days with 3 M acetic acid as the catalyst, and the final product was a reddish powder (see synthesis details in Materials and Methods section). The product exhibited a peak at 1251 cm^{-1} under FT-IR analysis (Figure S1), characteristic of an enamine bond, and the TPG CHO stretching peak at 1691 cm^{-1} disappeared. The sample exhibited excellent crystallinity and PXRD spectra (Figure S2) consistent with previous reports[14] and the simulated spectra (Figure S2). Nitrogen sorption measurements (Figure S3) showed that COF-Tp was a microporous material with a Brunauer−Emmett−Teller (BET) surface area of 111 $m^2\ g^{-1}$, and scanning electron microscopy (SEM) micrographs revealed a morphology of aggregated, disordered macroparticles (Figure S4).

To test for the transformation of LP-1 into COF-Tp, we systematically varied the amount of the TPG monomer added in a reaction with LP-1 and characterized the changes in material crystallinity, porosity, chemistry, and morphology. LP-1 was reacted with either 0.7, 1, or 1.4 equivalents of TPG relative to aldehyde functionalities in LP-1 and under similar solvothermal synthesis conditions as the direct synthesis route (dioxane/mesitylene, v/v, 1/1, 3 M acetic acid, 120 °C, 7 days, details in the Materials and Methods section). The transformed samples were named COF-Tp-LP1-*X*, where *X* indicates the equivalents of TPG added.

First, PXRD analysis (Figure 2a) revealed clear changes in the crystalline peak positions after the transformation reaction for all equivalents of TPG tested, but only COF-Tp-LP1-1 exhibited crystalline features that reflected a complete transformation into COF-Tp. The PXRD spectra of COF-Tp-LP1-1 were most similar to that of COF-Tp produced through direct synthesis, most notably with an intense diffraction peak at 4.7° along with complete attenuation of the LP-1 crystalline peak at 20.51°. For COF-Tp-LP1-0.7, the PXRD exhibited only a weak peak at 4.7° along with a residual peak at 20.51°, indicating the incomplete conversion of LP-1. For COF-Tp-LP1-1.4, the LP-1 peak at 20.51° completely disappeared but the peak at 4.7° was also absent, suggesting that this transformation reaction did not produce COF-Tp. The FT-IR spectra for all transformed samples and for COF-Tp produced by direct synthesis were nearly identical but completely different from that of LP-1, and all transformed samples and COF-Tp from direct synthesis exhibited an enamine peak at 1251 cm^{-1} (Figure 2b). Nitrogen sorption isotherms (Figure 2c) revealed a large increase in the porosity of COF-Tp-LP1-1 relative to the LP1 starting material, while the porosities of COF-Tp-LP1-0.7 and COF-Tp-LP1-1.4 only increased slightly relative to LP1. COF-Tp-LP1-1 had a surface area of 376 $m^2\ g^{-1}$, much higher than all other transformed samples and even higher than that of COF-Tp prepared from the direct synthesis (111 $m^2\ g^{-1}$). This was unexpected, but prior studies[10] have similarly observed higher porosities in COF synthesized through the transformation of a crystalline starting material. Additionally, COF-Tp-LP1-1 featured a sharp N_2 uptake for low pressures ($P/P_0 < 0.01$) indicative of microporosity, while this feature was absent in the other transformed samples. Finally, the thermal stability of these products was studied by thermogravimetric analysis (TGA, Figure 2d). While LP-1 was very stable and only decomposed at temperatures near 500 °C, the TGA of the transformed samples and of COF-Tp revealed decomposition at lower temperatures, and the TGA curves for COF-Tp and for all transformed samples were similar.

We also investigated the morphology of LP-1 and the COF-TP-LP1-X series by SEM analysis (Figure 3). After the reaction with TPG, the initially orange LP-1 powders turned reddish and produced fiber-like solids. LP-1 was comprised only of large flakes (Figure 3a), while the converted products contained a mixture of flakes and fibers (Figure 3b−d), which were distinct from the morphology of COF-Tp produced via the direct synthesis (Figure S4). This may be due to the different growth mechanisms of the directly synthesized and transformed COF-Tp samples. Directly synthesized COF-Tp underwent an error-correcting process during the reaction of the starting monomers to produce the final crystalline and porous materials. Conversely, the transformed COF-Tp samples were produced through the gradual substitution of aldehyde linkers of the flake-like LP-1. This gradual substitution process retains some of the flake-like morphology in the final material.

https://dx.doi.org/10.1021/acs.chemmater.0c04237
Chem. Mater. 2021, 33, 413−419

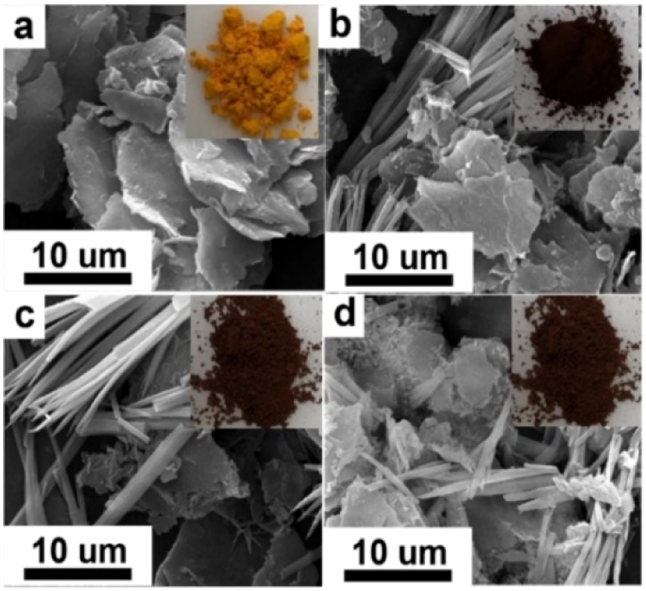

Figure 3. SEM images of (a) LP-1, (b) COF-Tp-LP1-0.7, (c) COF-Tp-LP1-1, and (d) COF-Tp-LP1-1.

Time-dependent experiments were conducted to obtain further insights into the transformation process from LPs into COFs. LP-1 and 1 equiv TPG were loaded in a series of sealed Pyrex tubes and heated at 120 °C for reaction times ranging from 1 to 7 days. While the direct synthesis of COF-Tp only takes 3 days, PXRD, FT-IR, and SEM measurements revealed that the transformation process took 7 days to complete. Time-dependent PXRD analysis (Figure 4a) revealed the slow emergence of a diffraction peak at 4.7°, which indicated that the linker substitution and transformation into COF-Tp took place over the course of 7 days. A weak peak at 4.7° appeared after one day, indicating that only a fraction of LP-1 had transformed into COF-Tp but with increased reaction time, the intensity of the peak at 4.7° gradually increased while the peak at 20.51° was attenuated and then completely disappeared. The transition process was also monitored by time-dependent FT-IR (Figure 4b), which revealed almost identical spectra for all aliquots taken. This indicates that the linker replacement reaction occurred within 1 day but that the further replacement, rearrangement, and crystallization process continued over longer reaction times. Finally, we also observed a morphology change from flakes to a mixture of flakes and fibers by time-dependent SEM (Figure 5), and the orange LP-1 solids also turned into reddish powders after one day and were unchanged visually with further reaction times (see insets in Figure 5).

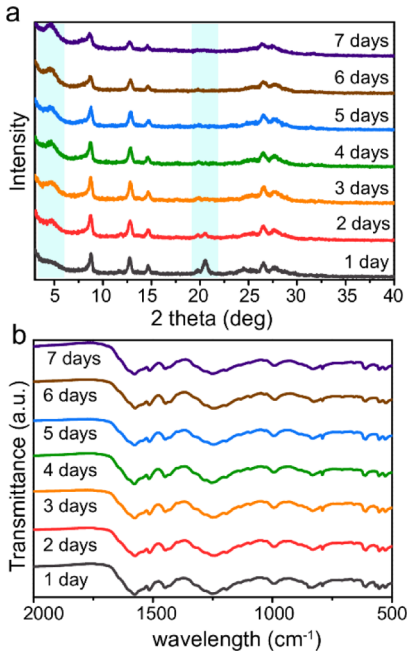

Figure 4. Time-dependent (a) PXRD and (b) FT-IR of COF-Tp-LP1-1 samples synthesized by the linker replacement strategy from LP-1.

To test the generality of this synthetic strategy and the effect of the linker size, we tested the transformation of linear polymer LP-2, which contained a much longer dialdehyde linker (4,4′-diformylbiphenyl, DFBP) compared to the linker present in LP-1 and the size of TPG. LP-2 was synthesized and isolated as an insoluble yellow powder, and the product exhibited similar PXRD peaks as LP-1 (Figure 6a). FT-IR (Figure 6b) revealed a peak at 1619 cm^{-1} corresponding to imine functional groups, and nitrogen sorption isotherms reflected a low BET surface area (Figure 6c). The transformation reaction was tested with 0.7, 1.0, and 1.4 equiv of TPG to the aldehyde linker in LP-2, and PXRD analysis revealed the successful transformation of LP-2 to COF-Tp when 1 equiv of TPG was used in the linker substitution reaction. COF-Tp-LP2-1 exhibited a strong diffraction peak at 4.7° and no features at 20.54° (Figure 6a), which is a characteristic of LP-2. FT-IR (Figure 6b) revealed significant compositional changes and indicated the formation of an enamine linkage with an absorption peak near 1251 cm^{-1}. The resulting TGA curves were similar to those for direct-synthesis COF-Tp (Figure 6d), and a similar morphology change from flakes to fibers was observed through SEM micrographs (Figure S5).

Time-dependent analysis of the changes in crystallinity, chemistry, and morphology was also conducted on the COF-Tp samples produced from the transformation of LP-2. Similar to the COF-Tp-LP1-1 samples, the transformation took place over several days as reflected by the gradual emergence of a diffraction peak at 4.7° over 7 days along with the disappearance of the LP-2 peak at 20.54° (Figure S6a). The FT-IR spectra also did not change after 1 day of reaction time and were identical to that of COF-Tp produced through the direct synthesis (Figure S6b). Finally, COFs transformed from LP-2 exhibited a similar fiber-like morphology (Figures S5, S7) as those prepared from the transformation of LP-1, indicating a similar growth mechanism.

To understand the importance of TPG as a linker substituent, we tested the transformation of LP-1 using different multifunctional aldehydes and multifunctional amines with a similar structure to TPG but lacking hydroxyl functional groups (Schemes S2 and S3). Prior studies reported the successful implementation of different linker substituents to achieve transformations from amorphous COPs to crystalline COFs,[5] between different COF structures with different dimensionalities,[12] and between COFs using different linkers.[6] However, our tests with these alternative linker substituents were unsuccessful. PXRD spectra after reactions with different amounts of the alternative aldehyde or amine remained identical with LP-1 or LP-2, implying that no transformation

https://dx.doi.org/10.1021/acs.chemmater.0c04237
Chem. Mater. 2021, 33, 413−419

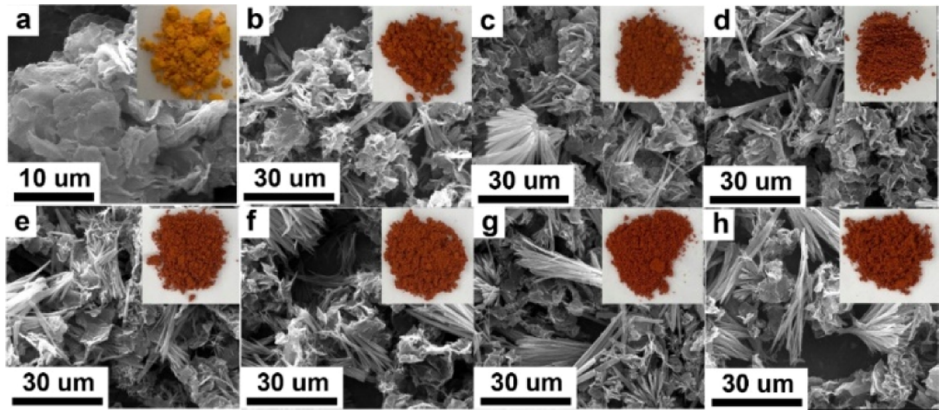

Figure 5. Time-dependent SEM images of COF-Tp-LP1-1 from 1 to 7 days (from a to f).

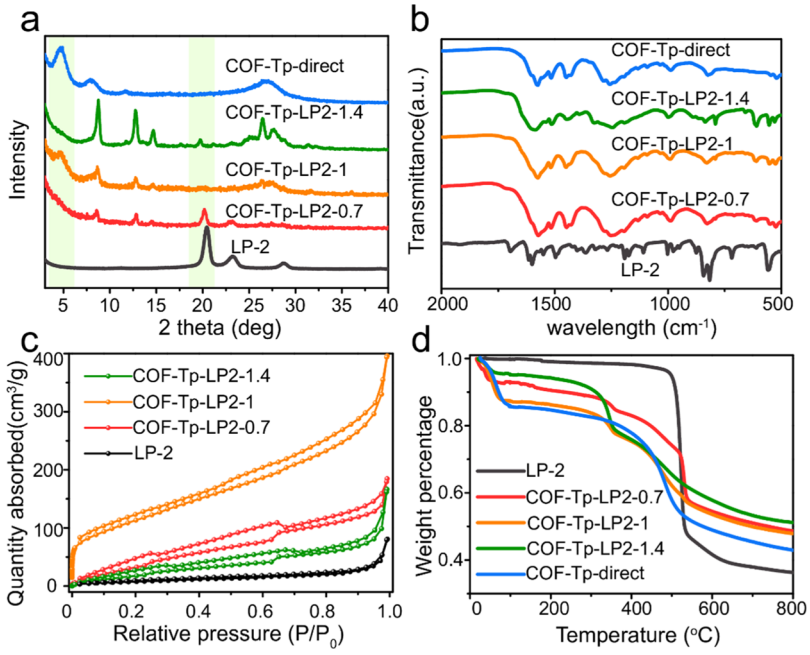

Figure 6. (a) PXRD, (b) FT-IR, (c) nitrogen sorption isotherms, and (d) TGA of LP-2, COF-Tp from direct synthesis, and samples synthesized by LP-2 reacting with different equivalents of TPG.

occurred (Figures S8 and S9). This demonstrates the importance of the tautomerization reaction in producing a thermodynamically stable product and driving the transformation reaction forward. Unlike TPG, the alternative substituents tested could not undergo a tautomerism after substitution because of a lack of a hydroxyl group ortho to the aldehyde functionality. This also demonstrates that LP-1 and LP-2 are stable under the solvothermal reaction conditions, except when the TPG monomer is present. The LP-1 and LP-2 materials do not fragment into soluble building blocks or monomers prior to forming the COF because otherwise the preparation of different COFs using alternative linker substituents would be possible. Our studies show that this does not happen, and therefore, the transformation of LP-1 or LP-2 into COF-Tp occurs through direct substitution rather than through the formation of soluble monomers as intermediates.

CONCLUSIONS

In summary, we demonstrated the transformation of 1D linear polymers into 2D COFs through sequential reversible and irreversible chemistries. Our strategy involved linker replacement with the monomer TPG, which produced a final COF product with improved crystallinity and greater porosity compared with samples produced using monomers as starting reagents. The enol-form intermediate rapidly underwent tautomerism after linker replacement, resulting in more stable ketone linkages for the final product. Analysis of the time-dependent changes in crystallinity, morphology, and chemistry demonstrated that linker replacement occurred quickly, within 1 day, but it took up to 7 days to complete the replacement and produce highly crystalline structures. We are currently extending this work to produce fully soluble linear polymers that can be solution-processed and subsequently transformed into a COF. This work provides insights into the dynamic nature of COFs and provides a novel potential approach to solution process COFs using linear polymers, which can be subsequently converted to COFs.

https://dx.doi.org/10.1021/acs.chemmater.0c04237
Chem. Mater. 2021, 33, 413−419

MATERIALS AND METHODS

Chemicals. All chemicals were purchased from commercial sources and used without further purification. PDA and TPA were purchased from Sigma-Aldrich; 4,4′-diformylbiphenyl (DFBP) was purchased from AmBeed; 1,3,5-tris(4-aminophenyl)benzene (TAPB) was purchased from TCI; 2,4,6-triformylphloroglucinol (TPG), benzene-1,3,5-tricarbaldehyde (BTCA), tetrakis(4-aminophenyl)-methane (TAPM), and 4′,4‴,4⁗,4⁗⁗⁗⁗-(ethene-1,1,2,2-tetrayl)-tetrakis[([1,1′-biphenyl]-4-carbaldehyde)] (ETTBC) were purchased from Jilin Chinese Academy of Sciences−Yanshen Technology Co., Ltd. Anhydrous dioxane, mesitylene, and *m*-cresol were purchased from Sigma−Aldrich. All other solvents used were purchased from Fisher Scientific.

Instrumentations and Characterizations. Supercritical CO_2 drying was conducted on a Leica EM CPD300 automated critical point dryer. COF powders were thoroughly washed using THF and a large excess of ethanol. Wet COF powders were loaded in tea bags (ETS drawstring tea filters, sold by English Tea Store, Amazon.com), immersed in pure ethanol, and then transferred into the drying chambers with the addition of an appropriate amount of pure ethanol. Using an automated procedure, the chamber was first cooled down to 14 °C and then supercritical CO_2 was introduced and exchanged with the solvent in the chamber over 12 cycles. The chamber was then warmed to 35 °C before the chamber was rapidly depressurized to release CO_2 gas. PXRD data were recorded on a Rigaku SmartLab XRD from 2θ = 1° up to 30° with 0.02° increment. COF samples were leveled flat on zero background sample holders. FT-IR of all solid samples were tested using a ThermoNicolet iS10 FT-IR spectrometer with a diamond ATR attachment. The spectra were tested using 64 scans with a resolution of 4. The testing range was set from 4000 to 500 cm^{-1}. The spectra shown are uncorrected. Nitrogen sorption measurements were conducted on a Quantachrome Autosorb-iQ-MP/Kr BET Surface Analyzer. Samples after supercritical CO_2 drying were degassed at 120 °C to remove any possible residue CO_2 molecules and tested immediately. BET surface areas were determined using BET adsorption models included in instrument software (ASiQwin version 5.2). SEM was performed on a FEI Quanta 400 FESEM operating at 30.00 kV. Samples were prepared by dispersing COF powders in ethanol and dropping on clean aluminum sample holders. After drying for 24 h, samples were coated with a 10 nm gold using a Denton Desk V Sputter.

Synthesis of LPs (LP-1 and LP-2). LP-1 was synthesized through the polycondensation of PDA and TPA monomers. In detail, PDA and TPA (molar ratio = 1:1) were dissolved in *m*-cresol separately. After mixing, the reaction occurs immediately to produce orange solids. After reacting for 2 h, the precipitated solids were washed using THF and methanol several times and filtered. Next, the isolated solids were thoroughly washed by THF using a Soxhlet extractor for 24 h and dried under vacuum at 80 °C overnight to obtain the dry orange powders. LP-1 is insoluble in many common solvents including DMSO, DMF, 1,4-dioxane, THF, acetone, acetonitrile, chloroform, and methanol. LP-2 was synthesized following the same procedure except DFBP in place of TPA.

Direct Synthesis of COF-Tp. COF-Tp was synthesized through the polycondensation of PDA and TPG in a molar ratio of 3 to 2 (Scheme S1). In detail, PDA and TPG were weighed and dissolved in a mixture of 1.5 mL of dioxane and 1.5 mL of mesitylene in a Pyrex tube and sonicated for 10 min to mix them homogeneously. Then, 0.5 mL of 3 M acetic acid was added and the solution was sonicated for another 10 min. The tube was degassed through three freeze−pump−thaw cycles and evacuated to an internal pressure of 150 mTorr and flame-sealed. The sealed tubes were warmed to room temperature and transferred into an oven and heated at 120 °C for 3 days. The reddish powder was isolated and washed thoroughly using THF and ethanol. Finally, the wet samples were dried using supercritical CO_2 dryer.

Transformation Synthesis of COF-Tp from LPs. LP-1 or LP-2 and TPG were weighed and dissolved in a mixture of 1.5 mL of dioxane and 1.5 mL of mesitylene in a Pyrex tube and sonicated for 10 min to mix homogeneously. Then, 0.5 mL of 3 M acetic acid was added, and the solution was sonicated for another 10 min. The tube was degassed through three freeze−pump−thaw cycles, evacuated to an internal pressure of 150 mTorr, and flame-sealed. The sealed tubes were warmed to room temperature and transferred to an oven and heated at 120 °C for 7 days. A reddish powder precipitated out and were separated and washed thoroughly using THF and ethanol. Finally, the wet samples were dried using supercritical CO_2 dryer.

ASSOCIATED CONTENT

Supporting Information

The Supporting Information is available free of charge at https://pubs.acs.org/doi/10.1021/acs.chemmater.0c04237.

Reaction schemes, summary of BET surface areas, and additional characterization data (PDF)

AUTHOR INFORMATION

Corresponding Author

Rafael Verduzco − *Department of Chemical and Biomolecular Engineering and Department of Material Science and NanoEngineering, Rice University, Houston, Texas 77005, United States;* orcid.org/0000-0002-3649-3455; Email: rafaelv@rice.edu

Authors

Dongyang Zhu − *Department of Chemical and Biomolecular Engineering, Rice University, Houston, Texas 77005, United States;* orcid.org/0000-0002-3413-5419

Xiaoyi Li − *Department of Chemical and Biomolecular Engineering, Rice University, Houston, Texas 77005, United States*

Yilin Li − *Department of Chemical and Biomolecular Engineering, Rice University, Houston, Texas 77005, United States*

Morgan Barnes − *Department of Material Science and NanoEngineering, Rice University, Houston, Texas 77005, United States*

Chia-Ping Tseng − *Department of Chemical and Biomolecular Engineering, Rice University, Houston, Texas 77005, United States;* orcid.org/0000-0003-4124-4223

Safiya Khalil − *Department of Chemical and Biomolecular Engineering, Rice University, Houston, Texas 77005, United States*

Muhammad M. Rahman − *Department of Material Science and NanoEngineering, Rice University, Houston, Texas 77005, United States;* orcid.org/0000-0003-1374-0561

Pulickel M. Ajayan − *Department of Material Science and NanoEngineering, Rice University, Houston, Texas 77005, United States;* orcid.org/0000-0001-8323-7860

Complete contact information is available at: https://pubs.acs.org/10.1021/acs.chemmater.0c04237

Notes

The authors declare no competing financial interest.

ACKNOWLEDGMENTS

The authors acknowledge financial support from the Army Research Laboratory (W911NF-18-2-0062) and the Welch Foundation for Chemical Research (C-1888). The authors also acknowledge Shared Equipment Authority at Rice University for access and utilization of characterization instruments.

REFERENCES

(1) Ding, S.-Y.; Wang, W. Covalent Organic Frameworks (COFs): From Design to Applications. *Chem. Soc. Rev.* **2013**, *42*, 548−568.
(2) Lohse, M. S.; Bein, T. Covalent Organic Frameworks: Structures, Synthesis, and Applications. *Adv. Funct. Mater.* **2018**, *28*, 1705553.
(3) Kandambeth, S.; Dey, K.; Banerjee, R. Covalent Organic Frameworks: Chemistry beyond the Structure. *J. Am. Chem. Soc.* **2019**, *141*, 1807−1822.
(4) Geng, K.; He, T.; Liu, R.; Dalapati, S.; Tan, K. T.; Li, Z.; Tao, S.; Gong, Y.; Jiang, Q.; Jiang, D. Covalent Organic Frameworks: Design, Synthesis, and Functions. *Chem. Rev.* **2020**, *120*, 8814−8933.
(5) Miao, Z.; Liu, G.; Cui, Y.; Liu, Z.; Li, J.; Han, F.; Liu, Y.; Sun, X.; Gong, X.; Zhai, Y.; Zhao, Y.; Zeng, Y. A Novel Strategy for the Construction of Covalent Organic Frameworks from Nonporous Covalent Organic Polymers. *Angew. Chem.* **2019**, *131*, 4960−4964.
(6) Zhai, Y.; Liu, G.; Jin, F.; Zhang, Y.; Gong, X.; Miao, Z.; Li, J.; Zhang, M.; Cui, Y.; Zhang, L.; Liu, Y.; Zhang, H.; Zhao, Y.; Zeng, Y. Construction of Covalent-Organic Frameworks (COFs) from Amorphous Covalent Organic Polymers via Linkage Replacement. *Angew. Chem., Int. Ed.* **2019**, *58*, 17679−17683.
(7) Smith, B. J.; Overholts, A. C.; Hwang, N.; Dichtel, W. R. Insight into the Crystallization of Amorphous Imine-Linked Polymer Networks to 2D Covalent Organic Frameworks. *Chem. Commun.* **2016**, *52*, 3690−3693.
(8) Qian, C.; Qi, Q.-Y.; Jiang, G.-F.; Cui, F.-Z.; Tian, Y.; Zhao, X. Toward Covalent Organic Frameworks Bearing Three Different Kinds of Pores: The Strategy for Construction and COF-to-COF Transformation via Heterogeneous Linker Exchange. *J. Am. Chem. Soc.* **2017**, *139*, 6736−6743.
(9) Waller, P. J.; AlFaraj, Y. S.; Diercks, C. S.; Jarenwattananon, N. N.; Yaghi, O. M. Conversion of Imine to Oxazole and Thiazole Linkages in Covalent Organic Frameworks. *J. Am. Chem. Soc.* **2018**, *140*, 9099−9103.
(10) Daugherty, M. C.; Vitaku, E.; Li, R. L.; Evans, A. M.; Chavez, A. D.; Dichtel, W. R. Improved Synthesis of β-Ketoenamine-Linked Covalent Organic Frameworks via Monomer Exchange Reactions. *Chem. Commun.* **2019**, *55*, 2680−2683.
(11) Zhang, G.; Tsujimoto, M.; Packwood, D.; Duong, N. T.; Nishiyama, Y.; Kadota, K.; Kitagawa, S.; Horike, S. Construction of a Hierarchical Architecture of Covalent Organic Frameworks via a Postsynthetic Approach. *J. Am. Chem. Soc.* **2018**, *140*, 2602−2609.
(12) Li, Z.; Ding, X.; Feng, Y.; Feng, W.; Han, B.-H. Structural and Dimensional Transformations between Covalent Organic Frameworks via Linker Exchange. *Macromolecules* **2019**, *52*, 1257−1265.
(13) Qian, H.-L.; Li, Y.; Yan, X.-P. A Building Block Exchange Strategy for the Rational Fabrication of de Novo Unreachable Amino-Functionalized Imine-Linked Covalent Organic Frameworks. *J. Mater. Chem. A* **2018**, *6*, 17307−17311.
(14) Kandambeth, S.; Mallick, A.; Lukose, B.; Mane, M. V.; Heine, T.; Banerjee, R. Construction of Crystalline 2D Covalent Organic Frameworks with Remarkable Chemical (Acid/Base) Stability via a Combined Reversible and Irreversible Route. *J. Am. Chem. Soc.* **2012**, *134*, 19524−19527.
(15) Karak, S.; Kandambeth, S.; Biswal, B. P.; Sasmal, H. S.; Kumar, S.; Pachfule, P.; Banerjee, R. Constructing Ultraporous Covalent Organic Frameworks in Seconds via an Organic Terracotta Process. *J. Am. Chem. Soc.* **2017**, *139*, 1856−1862.
(16) Sasmal, H. S.; Halder, A.; Kunjattu H, S.; Dey, K.; Nadol, A.; Ajithkumar, T. G.; Ravindra Bedadur, P.; Banerjee, R. Covalent Self-Assembly in Two Dimensions: Connecting Covalent Organic Framework Nanospheres into Crystalline and Porous Thin Films. *J. Am. Chem. Soc.* **2019**, *141*, 20371−20379.
(17) Han, X.; Zhang, J.; Huang, J.; Wu, X.; Yuan, D.; Liu, Y.; Cui, Y. Chiral Induction in Covalent Organic Frameworks. *Nat. Commun.* **2018**, *9*, 1294.
(18) Sun, Q.; Aguila, B.; Ma, S. A Bifunctional Covalent Organic Framework as an Efficient Platform for Cascade Catalysis. *Mater. Chem. Front.* **2017**, *1*, 1310−1316.
(19) Yang, Y.; Faheem, M.; Wang, L.; Meng, Q.; Sha, H.; Yang, N.; Yuan, Y.; Zhu, G. Surface Pore Engineering of Covalent Organic Frameworks for Ammonia Capture through Synergistic Multivariate and Open Metal Site Approaches. *ACS Cent. Sci.* **2018**, *4*, 748−754.
(20) Segura, J. L.; Royuela, S.; Mar Ramos, M. Post-Synthetic Modification of Covalent Organic Frameworks. *Chem. Soc. Rev.* **2019**, *48*, 3903−3945.
(21) Suematsu, K.; Nakamura, K.; Takeda, J. Polyimine, a C=N Double Bond Containing Polymers: Synthesis and Properties. *Polym. J.* **1983**, *15*, 71−79.
(22) Grätz, S.; Borchardt, L. Mechanochemical Polymerization − Controlling a Polycondensation Reaction between a Diamine and a Dialdehyde in a Ball Mill. *RSC Adv.* **2016**, *6*, 64799−64802.

https://dx.doi.org/10.1021/acs.chemmater.0c04237
Chem. Mater. 2021, 33, 413−419